

Electronic Supplementary Information

**Development of conductive Poly(vinyl alcohol) polymer using
Co(II)Li(I)-enriched metallohydrogel filler for soft
electrochemical applications**

Bharat Kumar Sahu, Gaurav Tiwari, Sakshi Tiwari and Mrigendra Dubey*

*Soft Materials Research Laboratory, Department of Metallurgical Engineering and Materials
Science, Indian Institute of Technology Indore, Indore-453552, India*

**Email: mdubey@iiti.ac.in*

<u>Table of Contents:</u>	<u>Pages</u>
Materials and Physical Methods	S2
Rheology Study	S2
EIS Study	S3
Synthesis and Characterization	S4
Scheme S1	S5
Figure S1	S5
Figure S2	S6
Figure S3	S6
Figure S4	S7
Figure S5	S7
Figure S6	S8
Figure S7	S9
Figure S8	S9
Figure S9	S10
Figure S10	S10
Figure S11	S11
Figure S12	S12
Figure S13	S13
Figure S14	S14
Figure S15	S14
Figure S16	S14
Figure S17	S15
Figure S18	S15
Reference	S16

Experimental Section

Materials and Physical Methods:

Reagents and solvents used in the current research work were procured from Finar Ltd, Ahmedabad, India, S. D. Fine Chem. Ltd., Mumbai, India and used as received without further purification. Methanol was purchased from Avantor Performance Indian Pvt. Ltd., Navi Mumbai India. Lithium hydroxide and 5-aminosalicylic acid were procured from Spectrochem Pvt. Ltd., Mumbai (India). $\text{Co}(\text{CH}_3\text{COO})_2 \cdot 4\text{H}_2\text{O}$ and Terephthaldehyde were purchased from Sigma-Aldrich, Mumbai (India). Polyvinyl Alcohol polymer (MW=115000) was purchased from Loba Chemie Pvt. Ltd., Jehangir Vill, Mumbai, India.

A UV-Vis absorption studies were carried out using PerkinElmer's spectrophotometer. PerkinElmer's spectrum two spectrometer was used to record FT-IR data. ^1H NMR spectrum was acquired on an AVANCE III 400 and 500 Ascend Bruker BioSpin International AG spectrometer. FE-SEM images were captured by JOEL-7610 F Plus. Powder XRD data was recorded on Rigaku SmartLab between angles $2\theta = 5-80^\circ$. TGA experiment was performed using PerkinElmer's STA 8000 simultaneous thermal analyser within the temperature range 30-800 °C with the scan rate 5 °C/min. Anton Paar Physical MCR301 was used to perform the Rheological analysis. Raman spectra were recorded using a HORIBA-JY LabRAM-HR spectrometer. Surface area analysis was performed using Quanta chrome, Autos orb iQ2 by Anton paar.

FE-SEM sample preparation:

A freshly prepared STL-Co metallohydrogel and STL-Co-PVA composite gel were drop casted on an FTO glass and dried between 30-45°C temperature under a vacuum desiccator for 48 hours to obtain dried STL-Co and STL-Co-PVA xerogels. Next, the obtained xerogel was coated with gold and mounted to the scanning electron microscope for morphological analysis.

Rheological Study:

Rheological experiments were carried out with the help of a rheometer MCR 301, Anton Paar, equipped with stainless steel parallel plates with dimensions 25 mm in diameter and a 0.5 mm gap. Experiments were conducted on freshly prepared gels (2% w/v). Dynamic amplitude sweep experiments were performed to obtain the linear viscoelastic region (LVR) of the metallohydrogel (STL-Co) and STL-Co-PVA composite gel by determining the storage modulus (G') and the loss modulus (G'') as a function of stress and strain at constant frequency 10 rad/sec, respectively. Dynamic oscillatory frequency sweep was performed at 23 °C (0.1 to 100 rad/sec) at a fixed shear strain of 1%. A time oscillatory strain sweep (Thixotropic)

experiment was conducted at a periodic low strain of 1% and high strain of 100% at a constant frequency of 10 rad/sec.

Electrochemical impedance spectroscopic (EIS) measurements

Nyquist, Bode impedance plots and DC current vs time characteristic curve

All electrochemical impedance measurements were performed at room temperature. Freshly synthesised STL-Co metallogel and STL-Co-PVA composite gel were casted into a circular shape disc with a diameter of 1.1 cm and a thickness of 0.5 cm.¹⁻² The circular-shaped disc used for the electrochemical impedance spectroscopy (EIS) measurements was fabricated using borosilicate glass. Borosilicate glass was selected due to its chemical inertness, thermal stability, and compatibility with the metallogel system, ensuring reliable and reproducible EIS measurements.

Nyquist and Bode impedance plots for STL-Co metallogel and STL-Co-PVA composite gel were recorded using a CH Instruments CHI604E electrochemical workstation within the frequency range 10^6 Hz to 10^{-2} Hz by applying a sinusoidal voltage of 10 mV. Further, the obtained Nyquist plot was fitted with a suitable equivalent electrical circuit model using EIS Analyzer software (Zsim).³⁻⁴

Ionic and electronic conductivity measurements

The ionic conductivity of STL-Co metallogel was measured from the conductivity (σ) vs frequency plots (Fig. S14). To obtain σ vs frequency plot, the Z' (real component of impedance) vs frequency data were processed by the following equation-

$$\sigma = \frac{1}{R} \cdot \frac{d}{A} \dots \dots \dots (1)$$

Where, R is the resistance of the STL-Co metallogel, d is the distance between two electrodes, and A is the electrode surface area.² In the σ vs frequency plot, the conductivity of STL-Co metallogel was measured by varying the frequency (Fig. S14).⁵⁻⁶

Transport number evaluation

The ionic transport number (t_{Li^+}) was calculated using the d.c. Polarization technique. The electrochemical cell SS| (STL-Co Metallogel) |SS (SS - stainless steel electrode) was polarized with an applied step potential of 0.75V, and the resulting current was acquired as a function of time, as shown in Fig. S15. The value of t_{Li^+} was calculated using the Vincent–Evans equation:

$$t_{Li+} = \frac{I_s(\Delta V - I_0 R_0)}{I_0(\Delta V - I_s R_s)} \dots\dots\dots (2)$$

Where, I_0 and I_s are the initial and steady-state currents, respectively. R_0 and R_s are the cell resistance before and after the polarization experiment obtained with the help of the Nyquist impedance plot. ΔV represents the applied step potential.⁶

Band gap estimation:

UV-Vis spectroscopy to obtain an absorption spectrum. To estimate the band gap (E_g), we obtained Tauc's plot by processing UV-Vis data by following Tauc's equation-

$$(\alpha h\nu)^2 = (h\nu - E_g) \dots\dots\dots (3)$$

Where, α , h , ν and E_g represent the absorption coefficient, Planck's constant, frequency of light and optical band gap, respectively (Fig. S4).

Synthesis and characterization:

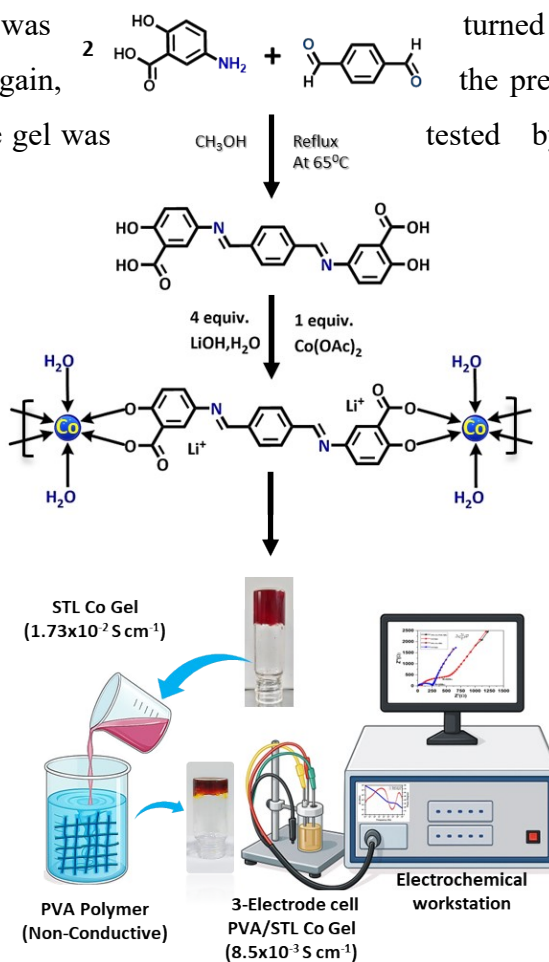
Gelator (STL): 5,5'-((1E,1'E)-(1,4-phenylene bis(methanylylidene)) bis(azanylylidene)) bis(2 hydroxybenzoic acid):

A methanolic solution of terephthalaldehyde (0.5 g, 3.727 mmol) was added dropwise to a solution of 5-aminosalicylic acid (1.141 g, 7.454 mmol), and the resulting solution was refluxed at 65 °C for 24 hours. The black-coloured solid compound was precipitated from the solution, which was further washed with methanol and diethyl ether; dried under vacuum. Yield 1.3 g (85%). Anal. calcd. for $C_{22}H_{16}N_2O_6$: C, 65.34; H, 3.99; N, 6.93; Found: C, 65.15; H; 3.70 N, 6.60. ¹H NMR ((CD₃)₂SO, 500 MHz, δ H, ppm) 7.04 (d, 2H, Ar-H), 7.61 (d, 2H, Ar-H), 7.78 (d, 2H, Ar-H), 8.06 (s, 4H, Ar-H), 8.78 (s, 2H, -HC=N), 10.09 (s, 2H, -OH), 11.79 (s, 2H, -COOH). ¹³C NMR ((CD₃)₂SO, 400 MHz, δ , ppm) 114.29, 116.31, 117.69, 124.31, 155.07, 172.19, 206.99.

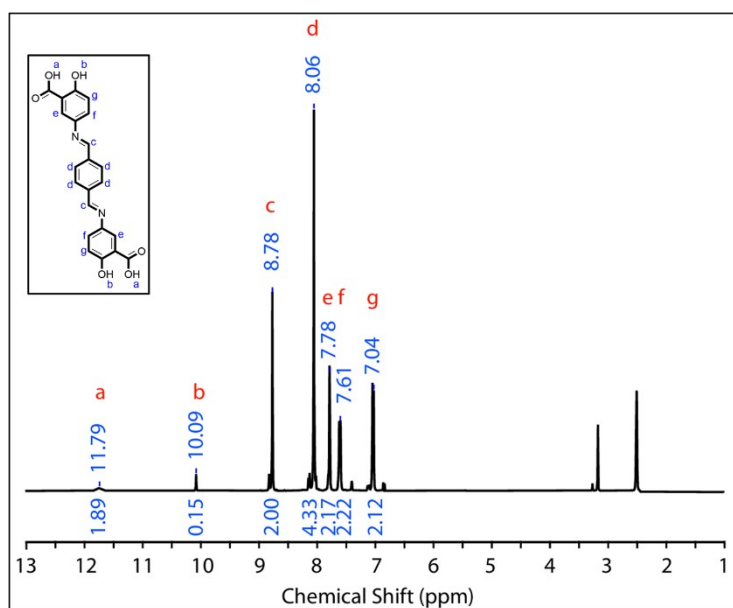
Synthesis of metallohydrogel STL-Co and STL-Co-PVA Composite gel

STL (20 mg, 0.049 mmol) was suspended in deionised water (0.5 mL) followed by the addition of LiOH.H₂O (8.30 mg, 0.197 mmol), and subsequent sonication of the mixture resulted in a dark red-coloured solution. A freshly prepared Co(OAc)₂•4H₂O (12.3 mg, 0.049 mmol) solution in deionised water (0.5 mL) was added to the above solution, which, upon sonication, resulted in a red-coloured metallohydrogel (STL-Co). The gel formation was primarily confirmed by the inverted vial test method. After that, the synthesised STL-Co metallo gel was mixed with PVA solution 1mL (3.48x10⁻⁴M) in an equal volume ratio (1:1), under sonication.

The resultant mixture was turned into a red colour STL-Co-PVA composite gel. Again, the preliminary gel formation of STL-Co-PVA composite gel was tested by the inverted vial method.

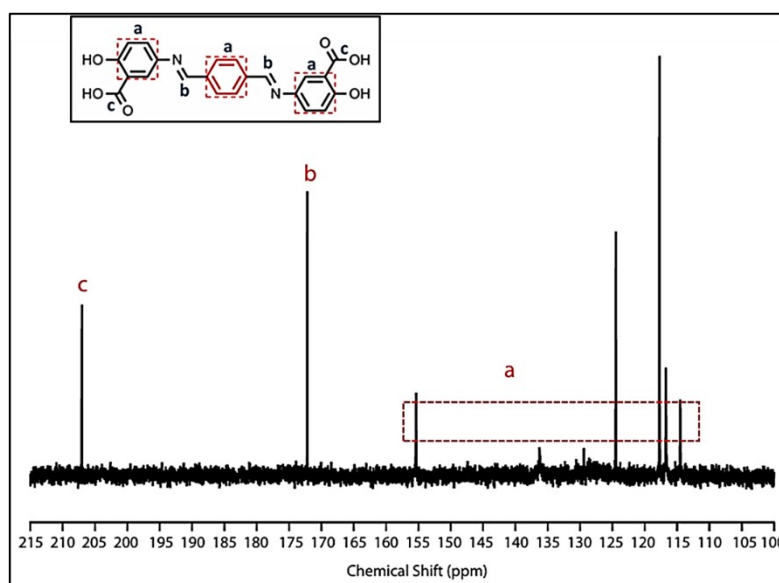


Scheme S1: adapted for the STL, STL-Co STL-Co-PVA along with the of the EIS test conductivity



Synthetic route of metallogel, and composite gel, demonstration setup for measurements.¹

Figure S1. ^1H -
spectrum of
(DMSO- d_6 , 500
MHz)
Note: The
appearance
of the additional
peaks
adjacent to the
aldimine and



NMR
STL
MHz)
appearance
peaks
aldimine and

aromatic protons (b to g) suggests the presence of conformers in trace amounts.⁷

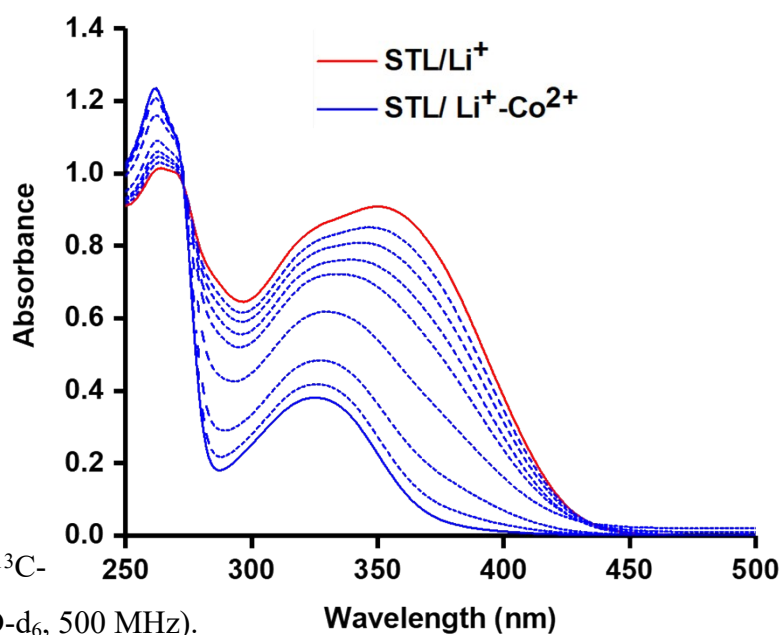


Figure S2. ^{13}C -
of STL (DMSO- d_6 , 500 MHz).

NMR spectrum

Figure S3. UV-Vis titration spectra of STL/ Li⁺ (1x10⁻⁴ M, H₂O, red line) vs Co²⁺ (1x10⁻² M, H₂O, blue lines) show an isosbestic point at 273 nm, which suggests the formation of a complex between deprotonated STL and Co²⁺.

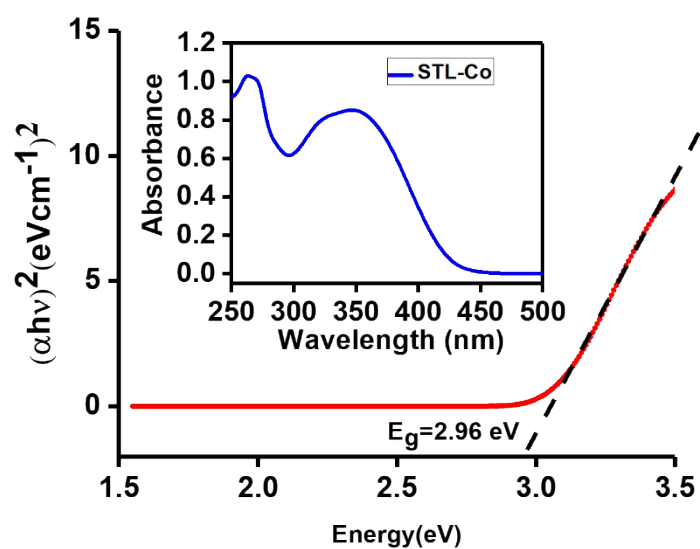


Figure S4. Tauc's plot for STL-Co metallogel and UV-Vis spectra (inset).

Note: Here the direct bandgap formula was employed to calculate the bandgap energy of the material using the Tauc relation $(\alpha h\nu)^2 = A(h\nu - E_g)$. This approach was selected based on the observed absorption behaviour and the band gap graph analysis of the metallogel system.

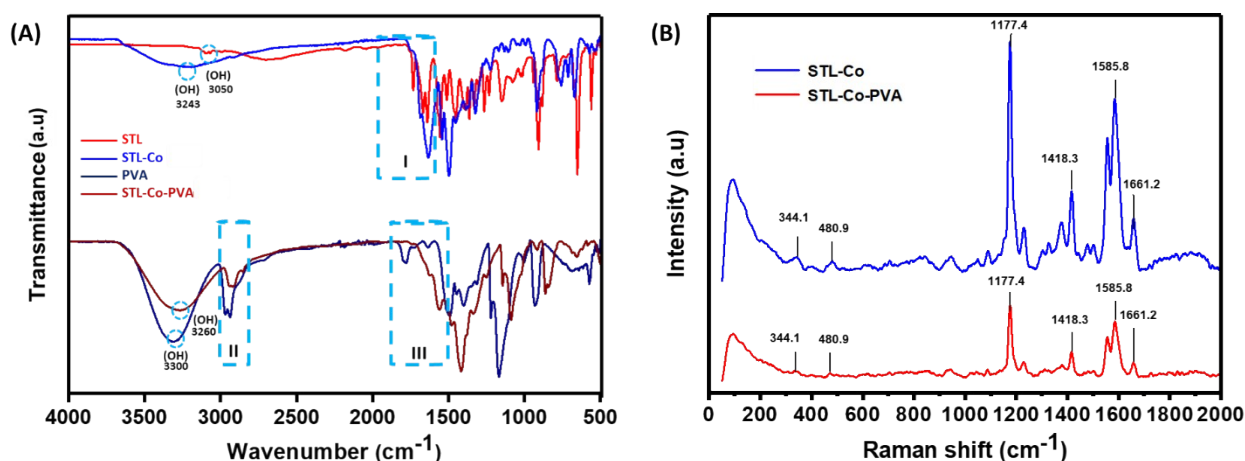


Figure S5. (A) FT-IR spectrum of STL gelator (red) shows ν (-OH) at 3050 cm⁻¹, and (I) ν (-C=O) at 1670, ν (-C=C) at 1610 cm⁻¹ and ν (-C=N) at 1570 cm⁻¹. FT-IR spectrum of STL-Co xerogel shows ν (-OH) at 3243 cm⁻¹, ν (-C=O) 1620, ν (-C=C) 1570 cm⁻¹ and ν (-C=N) 1560 cm⁻¹. Below blue spectrum of pure PVA ν (-OH) at 3260 cm⁻¹ shifted to ν (-OH) at 3300 cm⁻¹ ($\Delta\nu$ 40 cm⁻¹) for STL-Co-PVA polymer metallogel composite, perhaps due to hydrogen bonding between PVA matrix and STL-Co gel. The peaks at 1570 cm⁻¹ and at 1560 cm⁻¹, corresponding to ν (-C=C) and ν (-C=N), are present in the STL-Co-PVA polymer gel composite, suggesting better incorporation of STL-Co gel in the PVA matrix. (B) Raman spectrum of STL-Co metallogel (blue) and STL-Co-PVA composite gel (red) shows characteristic vibrational bands associated with the π -conjugated aromatic gelator and metal-ligand coordination. The prominent bands in the region of \sim 1200-1650 cm⁻¹ appear from aromatic C=C/C=N stretching vibrations (1580-1660 cm⁻¹) along with different -CH₂, -C-H vibrational modes (900-1450 cm⁻¹) confirming the presence of an extended aromatic conjugated backbone in the metallogel. In order, bands at 344.11 & 480.92 cm⁻¹ exhibited metal-ligand vibrational mode. Upon integration into the PVA matrix, the STL-Co-PVA composite retained spectral features of the metallogel, although with decreased intensity and slight broadening, indicating hydrogen bond formation between metallogel and PVA matrix without deformation of metallogel structure.

Note: Broadening of the -OH band in the FT-IR spectrum of STL-Co metallogel suggests the involvement of H₂O in the coordination complexes and, in turn, the formation of a gel.

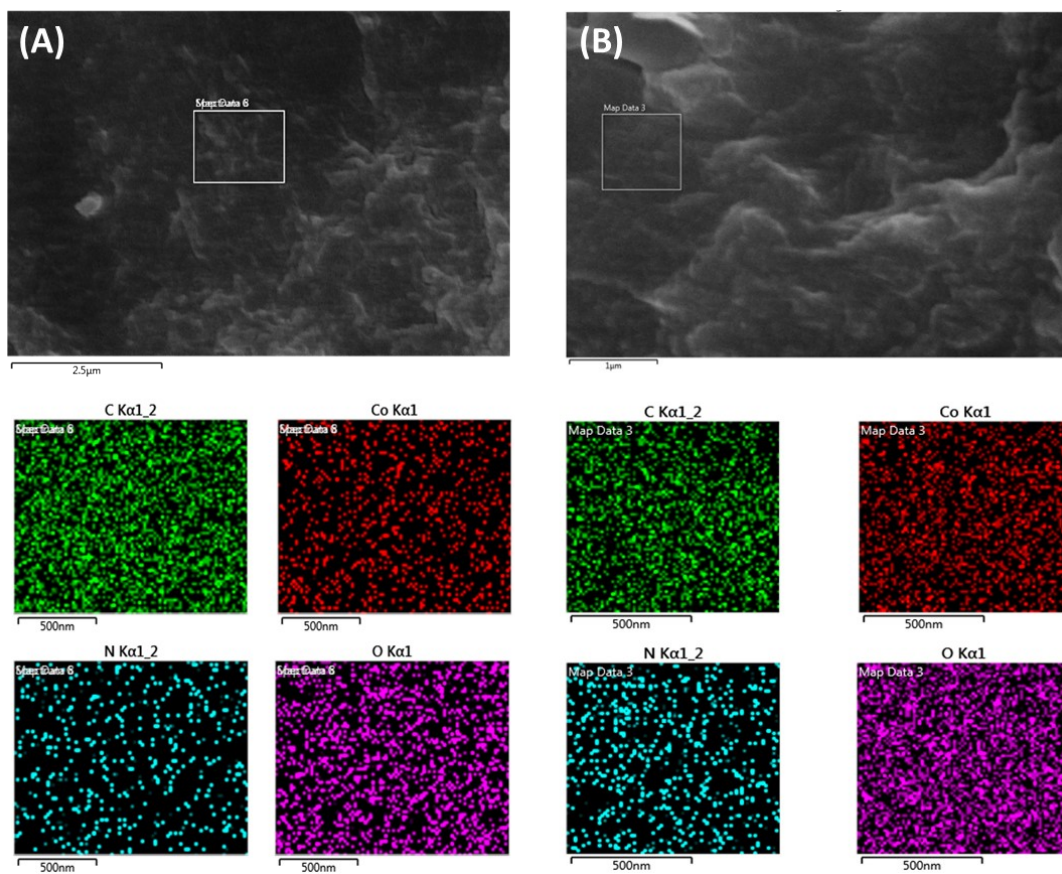


Figure S6. EDS mapping of (A) STL-Co xerogel and (B) STL-Co-PVA composite xerogel showing the uniform presence of C, O, Co and N elements.

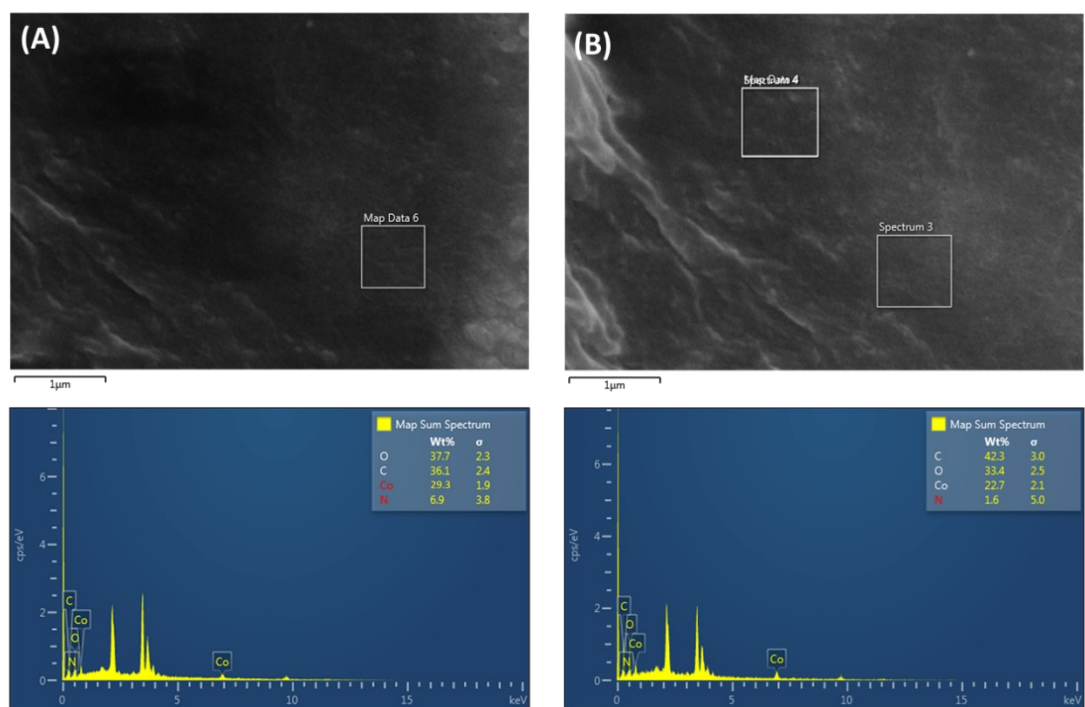


Figure S7. EDS elemental spectrum of (A) STL-Co xerogel and (B) STL-Co-PVA composite xerogel showing uniform distribution of C, O, Co and N elements.

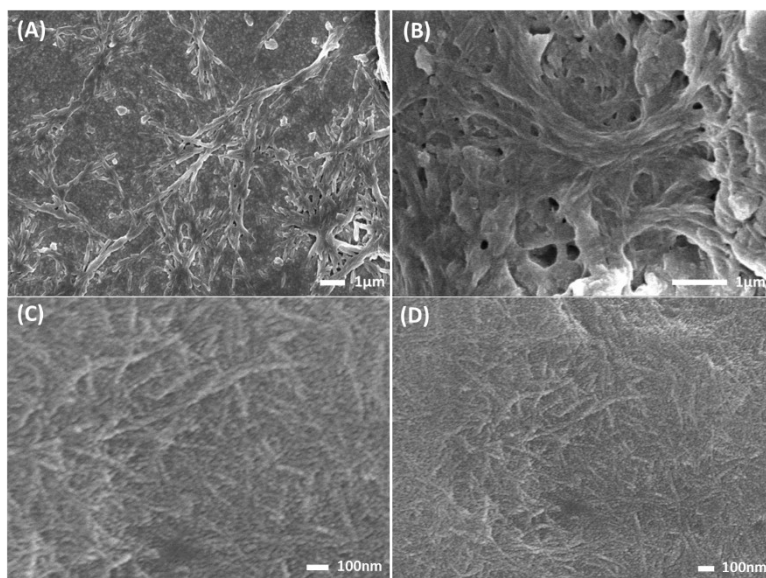


Figure S8. FE-SEM image of (A, B) STL-Co metallogel and (C, D) STL-Co-PVA polymer composite gel matrix.

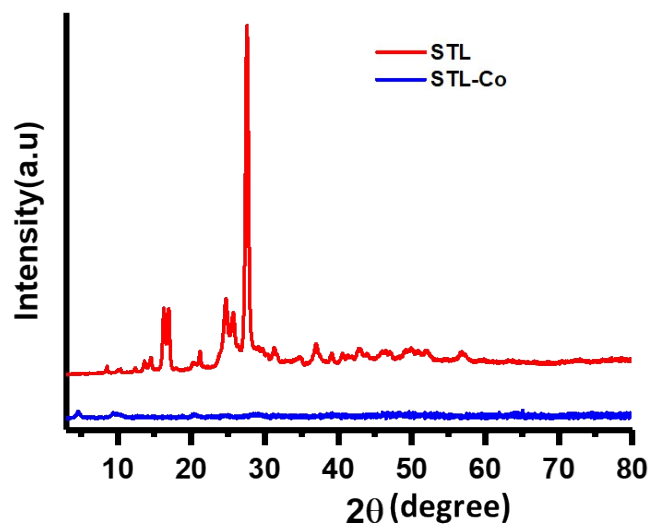


Figure S9. Powder XRD patterns of STL gelator and STL-Co xerogel.

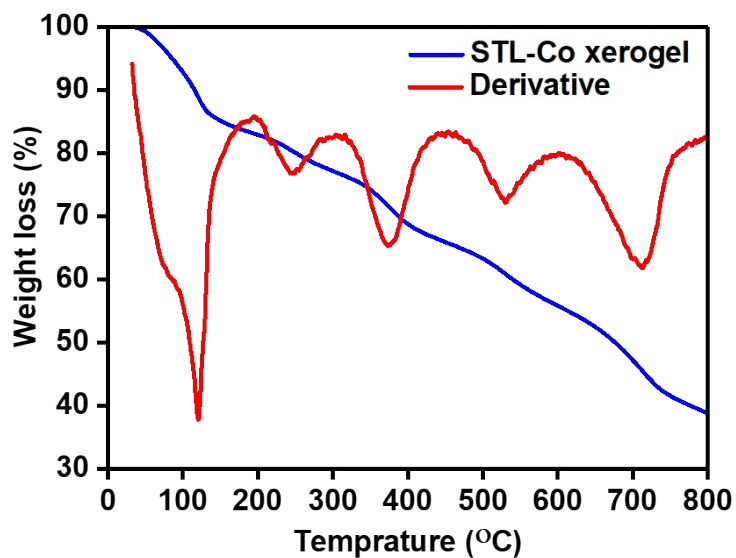


Figure S10. Thermogravimetric analysis for STL-Co xerogel, along with a derivative plot.

Note: The weight loss of STL-Co-xerogel within the temperature range of 30-300 °C is 25%. The weight loss in this temperature range is due to the removal of free and bound water molecules from the xerogel. Notably, initial weight loss of 9.62% up to the applied temperature of 100 °C is accredited to the removal of free water molecules, and further weight loss of 6.38% in the temperature range of 100-300 °C is due to the removal of bound water molecules, thus indicating the coordination of water molecules to the Co^{2+} .¹⁻²

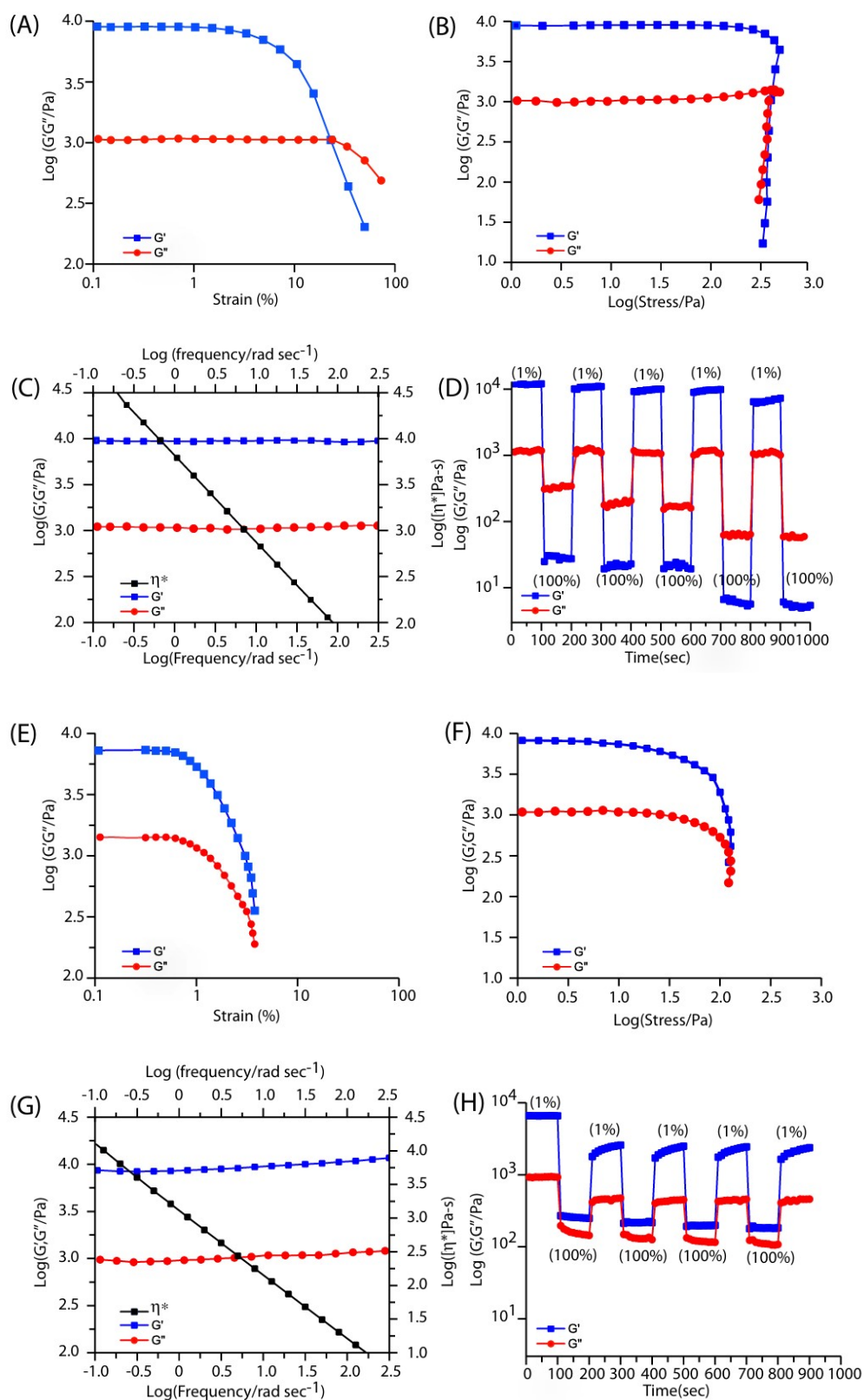


Figure S11. Rheological study with freshly prepared (A-D) STL-Co metallogel and (E-H) STL-Co-PVA composite gel matrix. Wherein, (A) Amplitude sweep strain and (B) Amplitude sweep stress of STL-Co metallogel showing variation in G' and G'' at a frequency of 10 rad s^{-1}

under 23 °C. (C) Double logarithmic plot showing the variation of G'' and G' against oscillatory frequency and complex viscosity, (D) Logarithmic plots of G' , G'' vs time at periodic strain of 1% and 100% of STL-Co metallogel.

Rheological experiments for STL-Co-PVA composite gel (E) Amplitude sweep strain and (F) Amplitude sweep stress of showing variation in G' and G'' at a frequency of 10 rad s^{-1} under 23 °C. (G) Double logarithmic plot showing the variation of G'' and G' against oscillatory frequency and complex viscosity, (H) Logarithmic plots of G' , G'' vs time at periodic strain of 1% and 100% of STL-Co-PVA composite gel.⁸

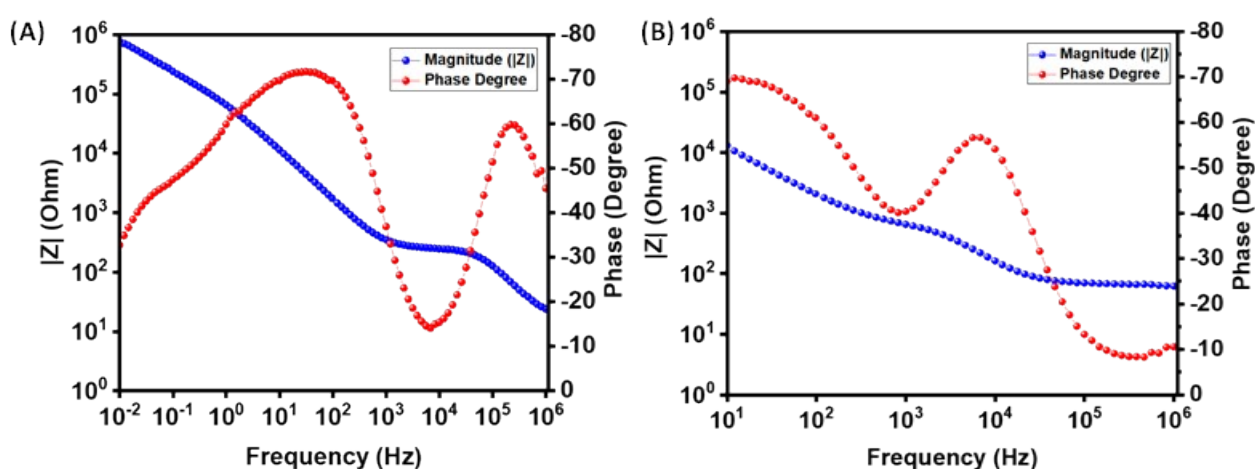


Figure S12. Bode impedance plots, left axis: Bode magnitude plot and right axis: Bode phase plot for (A) STL-Co metallogel, (B) STL-Co-PVA composite gel.

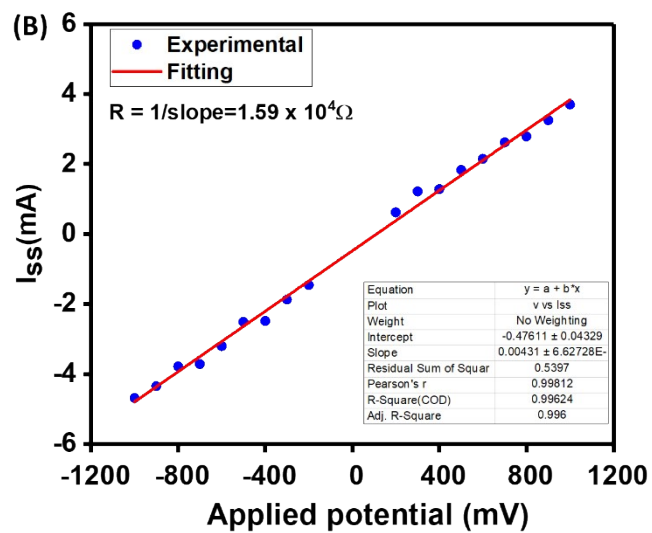
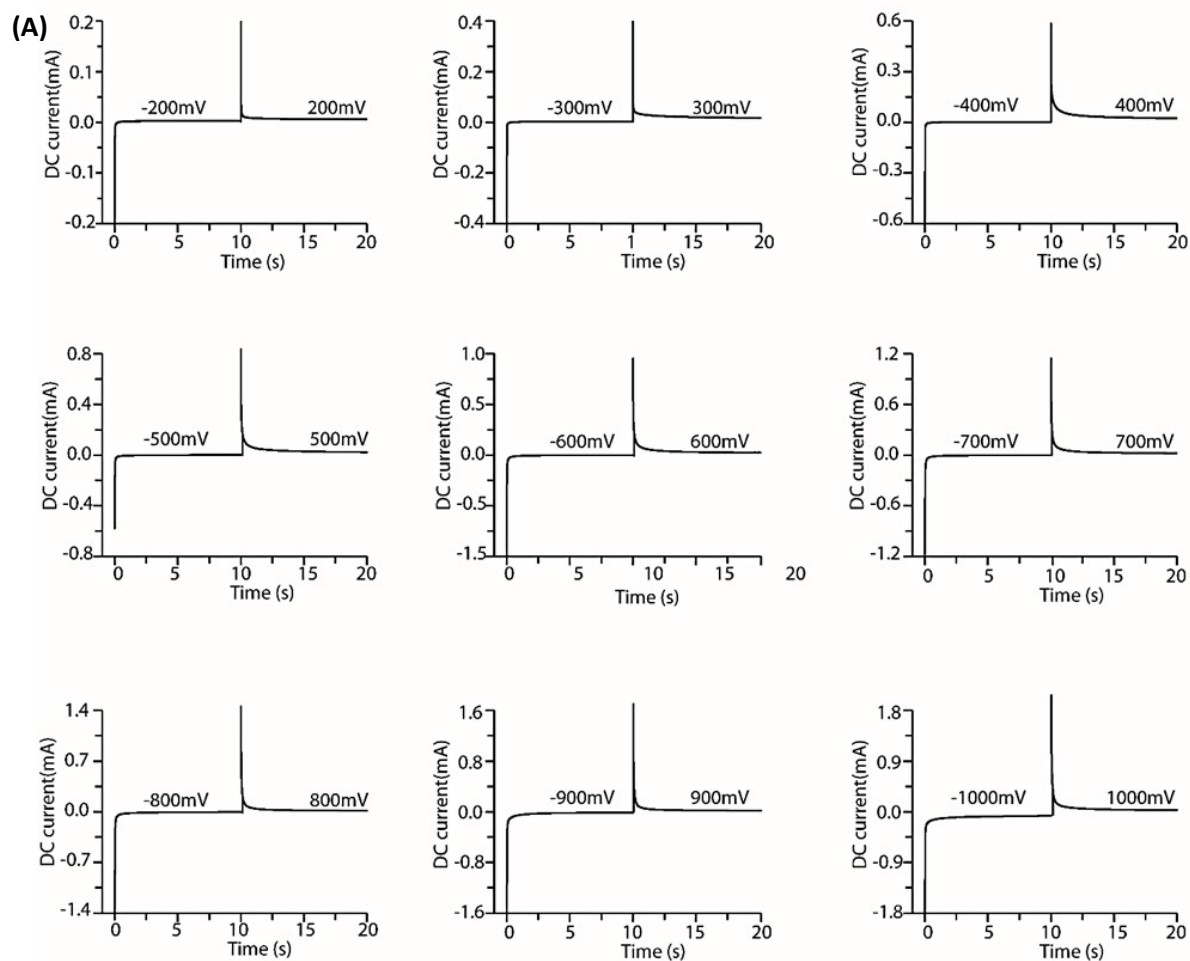


Figure S13. (A) DC current vs time curves at different applied DC potentials, (B) Steady state current (I_{ss}) vs applied potential plot, the experimental data follow Ohm's law.¹

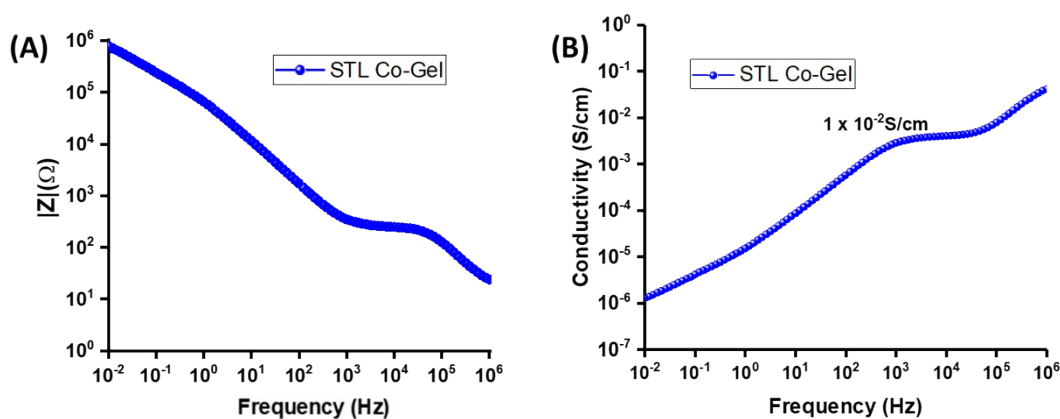


Figure S14. (A) Z vs frequency plot of STL-Co metallogel (B) Conductivity vs frequency plot of STL-Co metallogel.

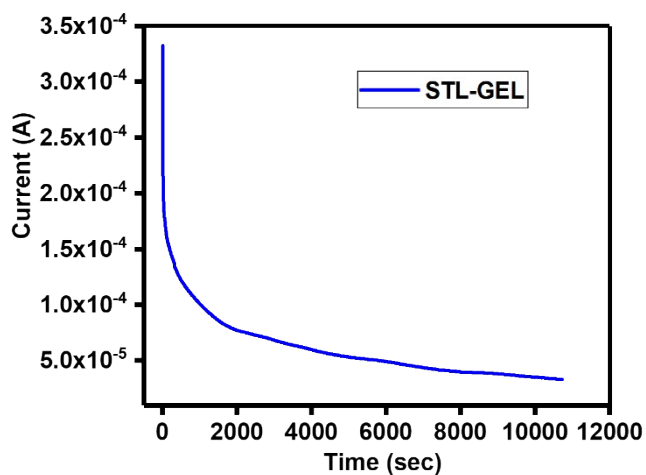


Figure S15. D.C. polarization curve of cell: SS|STL-Co -metalloel|SS with applied step potential of 0.75 V.⁵

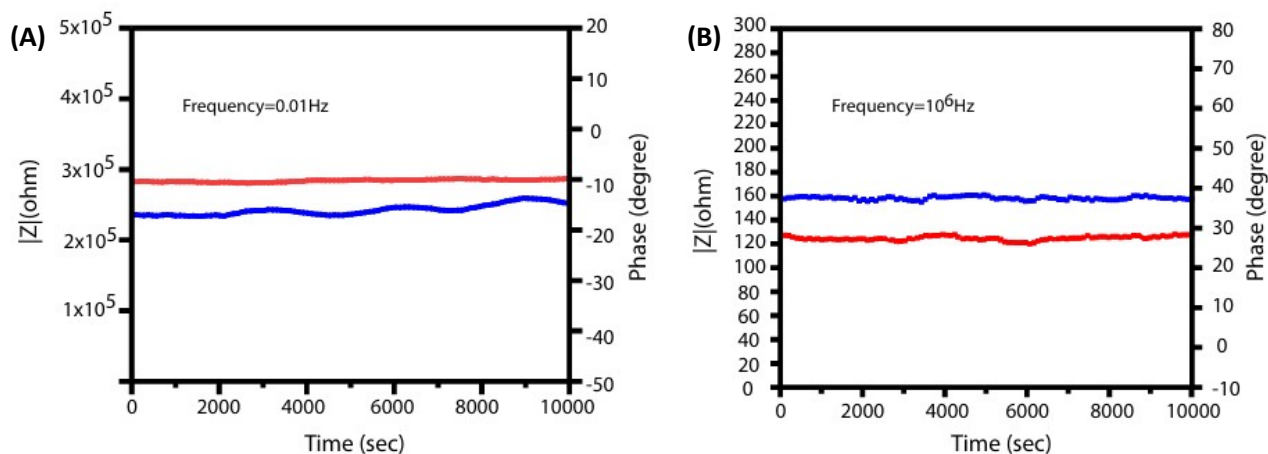


Figure S16. (A) Impedance variation with time at 0.01 Hz and (B) impedance variation with time at 10^6 Hz.

Note- Impedance of STL-Co metallogel was monitored for three hours, and it was observed that the impedance showed very slight variation against low and high frequency signals, thus revealing the electrically stable behaviour of STL-Co metallogel.^{1,6}

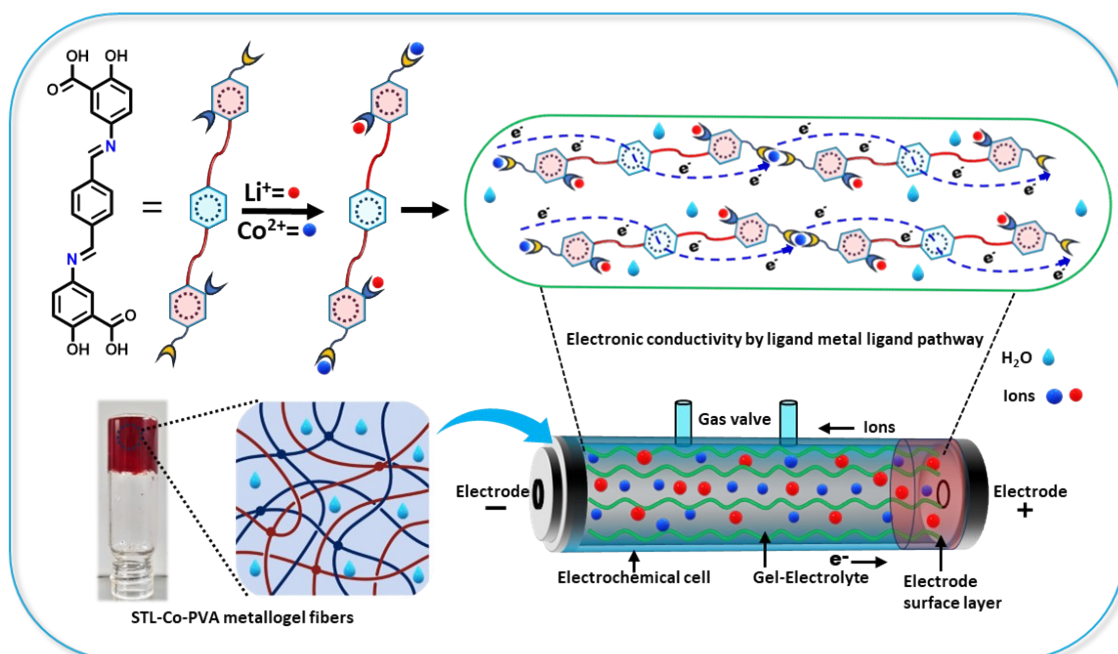


Figure S17. Schematic representation of proposed plausible mechanism for conducting behaviour of STL-Co-metallogel.

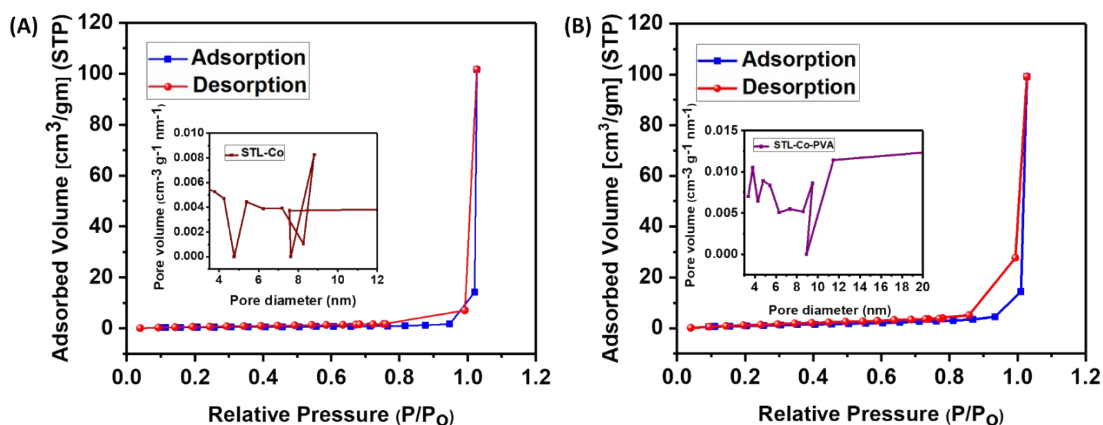


Figure S18. BET surface area analysis, N_2 adsorption/desorption isotherms with inset pore size distribution curve plot for (A) STL-Co metallogel, (B) STL-Co-PVA composite gel.⁹

References:

1. Y. Kumar and M. Dubey, *Chem. Commun.*, 2022, **58**, 549.
2. D. Rawlings et al., *Chem. Mater.*, 2021, **33**, 6464.
3. S. N. Patel, A. E. Javier, G. M. Stone, S. A. Mullin and N. P. Balsara, *ACS Nano*, 2012, **6**, 1589.
4. K. Nyamayaro, V. Triandafilidi, P. Keyvani, J. Rottler, P. Mehrkhodavandi and S. G. Hatzikiriakos, *Phys. Fluids*, 2021, **33**, 032010.
5. V. K. Pandey, M. K. Dixit, S. Manneville, C. Bucher and M. Dubey, *J. Mater. Chem. A*, 2017, **5**, 6211.
6. Y. Kumar, C. Mahendar, A. Kalam and M. Dubey, *Sustainable Energy Fuels*, 2021, **5**, 1708.
7. M. N. Chaur, D. Collado and J. M. Lehn, *Chem. Eur. J.*, 2011, **17**, 248.
8. C. Mahendar, M. K. Dixit, Y. Kumar and M. Dubey, *J. Mater. Chem. C*, 2020, **8**, 11008.
9. E. Elanthamilan, A. Sathiyam, S. Rajkumar, E. J. Sherylb and J. P. Merlin, *Sustainable Energy Fuels*, 2018, **2**, 811-819.